A Multi-slack Bus Model for Bi-directional Energy Flow Analysis of Integrated Power-gas Systems

Yujia Huang, Qiuye Sun, *Senior Member*, *IEEE*, Ning Zhang, and Rui Wang, *Senior Member*, *IEEE*

***Abstract*—The bi-directional energy conversion components such as gas-fired generators (GfG) and power-to-gas (P2G) have enhanced the interactions between power and gas systems. This paper focuses on the steady-state energy flow analysis of an integrated power-gas system (IPGS) with bi-directional energy conversion components. Considering the shortcomings of adjusting active power balance only by single GfG unit and the capacity limitation of slack bus, a multi-slack bus (MSB) model is proposed for integrated power-gas systems, by combining the advantages of bi-directional energy conversion components in adjusting active power. The components are modeled as participating units through iterative participation factors solved by the power sensitivity method, which embeds the effect of system conditions. On this basis, the impact of the mixed problem of multi-type gas supply sources (such as hydrogen and methane generated by P2G) on integrated system is considered, and the gas characteristics-specific gravity (SG) and gross calorific value (GCV) are modeled as state variables to obtain a more accurate operational results. Finally, a bi-directional energy flow solver with iterative SG, GCV and participation factors is developed to assess the steady-state equilibrium point of IPGS based on Newton-Raphson method. The applicability of proposed methodology is demonstrated by analyzing an integrated IEEE 14-bus power system and a Belgian 20-node gas system.**

***Index Terms*—Bi-directional energy flow analysis, integrated power-gas system (IPGS), multi-slack bus model, multi-type gas supply sources.**

I. Introduction

With the increase of renewable energy sources [1], the integrated power-gas systems (IPGS) have aroused extensive attention [2], [3]. On the one hand, the gas-fired generator (GfG) plays a major role in the integrated power-gas system because of its rapid response ability in peak regulation [4], [5]. On the other hand, power-to-gas (P2G) technology converts electric energy into hydrogen (H_2) or synthetic natural gas (SNG) which can not only regulate power with quicker ramp rates, but also can store the energy using an existing natural gas network [6], [7]. Therefore, the bi-directional energy conversion brought by GfG and P2G further enhances the interaction between power and gas systems.

Manuscript received August 21, 2022; revised November 20, 2022; accepted December 21, 2020. Date of online publication April 30, 2021; date of current version February 6, 2024.

Y. J. Huang, Q. Y. Sun (corresponding author, email: sunqiuye@ise.neu.edu.cn), N. Zhang, and R. Wang are with College of Information Science and Engineering, Northeastern University, Shenyang 110819, China.

DOI: 10.17775/CSEEJPES.2020.04190

There are several papers on studying the application of GfG and P2G units in the integrated power-gas systems in [8]–[12]. Reference [8] pointed out that the operational costs of the IPGS could be reduced by injecting H_2 into the gas network in a quantity and quality according to the gas safety regulations. Clegg and Mancarella [9] modelled the P2G units with power system requirements and developed an integrated model to exploration of the techno-economic, environmental, and operational implications of P2G units in IPGS. To find the best expansion plan with the lowest cost, reference [10] co-planned the GfG units with power systems in an integrated manner, and established an innovative capacity expansion collaborative planning (ECP) framework. In [11], a new real-time optimal scheduling algorithm for joint operation of the P2G and GfG units was proposed, which could not only arbitrage benefit, but also achieved a more stable return on investments by reliving the congestion in IPGS. In [12], an optimal day-ahead optimization schedule for IPGS with the P2G units is proposed, which can minimize the operation cost.

The research in the above papers relies on their energy flow analysis to determine the initial conditions, operating limits and so on. The energy flow can be divided into steady-state and transient calculation, where the steady-state calculation of energy flow is useful for long-term research(e.g. network planning, reliability assessment). Hence, it is reasonable to neglect the dynamic characteristics of gas flows [13]. Several papers on steady-state energy flow calculation can be found in [14]–[17]. In the energy flow algorithms of these studies, the slack bus selection can be divided into single slack bus (SSB) and distributed slack bus (DSB) model. But as said, the SSB model is considered a mathematical artifact for power flow analysis, without any direct link with the physical system [18]. Thus, in [14], [15] and [17], the DSB model with constant participation factors is used for the energy flow analysis, but the bi-directional energy conversion and the effect of system conditions on the participation factors are not considered. In [16], the bi-directional energy flow analysis with GfG and P2G units is studied, but the algorithm in this study assume a SSB model. It is worth noting that, in these studies, the slack buses of power systems are all served by the gas network loads, GfG units. However, the slack bus as gas load brings great burden to the gas network [19], which can lead to pressure changes and affect the final steady-state results of gas network [20]; And then, the safe operation limit of pressure in gas networks makes the slack bus limited power capacity, which is contradictory to the unlimited power of the slack bus to maintain power balance [21].

On the other hand, many countries have put forward policies using existing natural gas facilities to accept the injection of gas such as H_2 and methane which are generated by P2G [22]. But the injection and mixture of different composition gas sources can lead to changes in gas characteristics-specific gravity (SG) and gross calorific value (GCV). First, the SG as one of the elements in gas flow equation can affect not only the amount of volume flow in pipelines but also the pressure drop [23], [24]. Then, the gas with a lower GCV reduces the energy delivered to the loads when the same volume flow supplied [8], [9]. So the gas characteristics SG and GCV must be combined with the pressure level to jointly determine the operating state of the system that avoid the security of supply [8], and ensure the calculation of operational state values which can provide correct data for higher level research of IPGS [23]. Hence, the SG and GCV at each node must be modelled as variables in the gas state solution equation.

To the best of authors' knowledge, there is no consideration that the capacity limitation of slack bus and the concentrated burden of gas system brought by slack bus, and no clear modeling of gas characteristics in bi-directional steady-state energy flow analysis. To solve these problems, the main contributions of this paper can be concluded as follows.

1) A multi-slack bus model is proposed for integrated power-gas systems. The energy conversion components with adjustable active power outputs or inputs are modeled as participating units through participation factors by using the power sensitivity method, which can not only reduce the burden of slack bus but also reflect the effect of system conditions on participation factors.

2) The specific gravity and gross calorific value of gas are established as iterative variables for the first time in bi-directional energy flow analysis, which can consider the effect of multi-type gas supply sources mixture on systems to obtain a more accurate operation results.

3) A bi-directional energy flow solver with iterative participation factors, SG and GCV based on the Newton-Raphson method is developed to assess the steady-state equilibrium point of IPGS, which more realistically represents the interdependency of power and gas systems.

This paper is described in detail as follows. The proposed multi-slack bus model is described in Section II. The detailed gas flow, specific gravity and gross calorific value balance formulations are described in Section III. The interdependencies models between two systems and the integrated power flow solution based on Newton's method are described in Section IV. Finally, the case studies are carried out on the integrated IEEE 14-bus power system and a Belgian 20-node gas system in Section V, and conclusions are given in Section VI.

II. The Proposed Multi-slack Bus (MSB) Model

As mentioned in [9], P2G units can be modeled as equivalent generation units, that is, negative generation unit. Thus, this paper takes into account the advantages of energy conversion units (such as GfG units and emerging P2G technology) in adjusting active power. A multi-slack bus model established using participation factors for the energy conversion units with adjustable active power outputs or inputs. The participation factors are defined by the power sensitivity method, which are extended from traditional generators in power system [25] to energy conversion units in integrated power-gas systems.

A. Participation Factors Formulation

In the MSB model, energy conversion units jointly act as slack buses to remove the concentrated burden of systems. The MSB power flow analysis reclassifies the bus types into reference, slack, PV and PQ buses. The reference bus is the same as the slack bus of SSB power flow analysis. PV and PQ bus, which are also consistent with traditional power flow. The slack buses can be divided into $\tilde{P}V$ or $\tilde{P}Q$, respectively representing PV or PQ with adjustable active power to compensate the system active slack. Their actual outputs or inputs depends on the participation factors.

Participation factor ζ_i is the ratio of the active power contribution of participating unit i to the total active power slack, which is calculated by:

$$\zeta_i = \frac{\Delta P_i^{\text{slack}}}{\sum_i^{N_{\text{slack}}} \Delta P_i^{\text{slack}}} \tag{1}$$

$$\sum_i^{N_{\text{slack}}} \zeta_i = 1 \quad \forall i = 1, \cdots, N_{\text{slack}} \tag{2}$$

where N_{slack} is the total number of participating units. And the sum of all participation factors is one. Power sensitivity method is used to calculate participation factors for the participating units. The power balance equations are given by:

$$\Delta P_i = P_i^{\text{sp}} - \sum_{j=1}^{N_E} |V_i||V_j|(G_{ij}\cos\theta_{ij} + B_{ij}\sin\theta_{ij}) \tag{3}$$

$$\Delta Q_i = Q_i^{\text{sp}} - \sum_{j=1}^{N_E} |V_i||V_j|(G_{ij}\sin\theta_{ij} - B_{ij}\cos\theta_{ij}) \tag{4}$$

where P_i^{sp} and Q_i^{sp} are the specific active and reactive power values injected into bus i. $|V_i|$ and $|V_j|$ are voltage magnitudes of bus i and j while θ_{ij} is the difference of voltage angles θ_i and θ_j of bus i and j. G_{ij} and B_{ij} are electricity conductance and susceptance of transmission line ij, respectively. By expanding (3) and (4) with Taylor expansion and leaving the main terms, the initial linearized equation used to derive the participation factors can be written as (5).

$$\begin{bmatrix}\Delta\theta \\ \Delta V\end{bmatrix} = J^{-1}\begin{bmatrix}\Delta P \\ \Delta Q\end{bmatrix} \tag{5}$$

where $[\Delta\theta, \Delta V]^{\text{T}}$ are the vectors of voltage mismatches. J is Jacobin matrix consisting of the partial derivatives of P and Q to θ and V, respectively. Then, the mismatches ΔP can be separated into active power contribution ΔP^{slack} of participating units and load mismatches ΔP^{load}. ΔQ in the same way, but the energy conversion units usually only exchange active power with the electricity network, so ΔQ^{slack} are zero. Hence the linearized equation at slack buses are rewritten as:

$$\begin{bmatrix}\Delta\theta \\ \Delta V\end{bmatrix} = S_1\Delta P^{\text{slack}} + S_2\begin{bmatrix}-\Delta P^{\text{load}} \\ -\Delta Q^{\text{load}}\end{bmatrix} \tag{6}$$

Since the voltages and phase angles mismatches are zero [25] in the ideal state, (6) can be written as:

$$\Delta P^{\text{slack}} = -[S_1]^{-1} S_2 \begin{bmatrix} -\Delta P^{\text{load}} \\ -\Delta Q^{\text{load}} \end{bmatrix} \tag{7}$$

Consequently, the power sensitivity of participating units with respect to load mismatches can be represented by the power sensitivity matrix $\boldsymbol{S}$:

$$\boldsymbol{S} = -[S_1]^{-1} S_2 \tag{8}$$

where S_1 and S_2 are submatrices made up of the elements in J^{-1}. S_1 and S_2 are expressed by:

$$S_1 = \begin{bmatrix} J'_{1,1} & \cdots & J'_{1,N_{\text{slack}}} \\ \vdots & \ddots & \vdots \\ J'_{N_{\text{slack}},1} & \cdots & J'_{N_{\text{slack}},N_{\text{slack}}} \end{bmatrix} \tag{9}$$

$$S_2 = \begin{bmatrix} J'_{1,1} & \cdots & J'_{1,N_E+N_{\text{PQ}}} \\ \vdots & \ddots & \vdots \\ J'_{N_{\text{slack}},1} & \cdots & J'_{N_{\text{slack}},N_E+N_{\text{PQ}}} \end{bmatrix} \tag{10}$$

where N_{E} and N_{PQ} are the total number of buses and PQ buses in the electricity network. Through the power sensitivity matrix, we can calculate the power contribution ΔP^{slack} of participating units corresponding to the load mismatches. Then, the active power in the network can be assigned to participating units using power sensitivity matrix, and the participation factors in (1) can be calculated for each unit. Moreover, the effect of network parameters, topology or system conditions on the participation factors can be reflected through $\boldsymbol{S}$.

B. Multi-Slack Bus Model

By applying the participation factors calculated above, the variable active power of participating units at each slack bus i can be defined as:

$$P_i^{\text{slack}} = P_i^{\text{slack},0} + \zeta_i \tilde{P} \tag{11}$$

where $P_i^{\text{slack},0}$ is the set-point of active power of each participating unit. $\tilde{P}$ is active power slack.

When participating units are GfG units, (11) can be expressed as:

$$P_i^{\text{GfG}} = P_i^{\text{GfG},0} + \zeta_i \tilde{P} \tag{12}$$

When participating units are P2G units, (11) can be expressed as:

$$-P_i^{\text{P2G}} = -P_i^{\text{P2G},0} + \zeta_i \tilde{P} \tag{13}$$

It can be found that P_i^{GfG} and P_i^{P2G} are regulated during power flow solutions according to their assigned participation factors ζ_i and the active power slack $\tilde{P}$.

To ease the description, assuming that all GfG and P2G are participating units, then the nodal power flow equations are given by:

$$\Delta P_i = P_i^{\text{slack}} + P_i^{\text{gen}} - P_i^{\text{load}} - P_i^{\text{com}} - \sum P_{ij} = 0 \quad \forall i = 1, 2, \cdots, N_E \tag{14}$$

$$\Delta Q_i = Q_i^{\text{gen}} - Q_i^{\text{load}} - \sum Q_{ij} = 0 \quad \forall i = 1, 2, \cdots, N_{\text{PQ}} \tag{15}$$

where $\sum P_{ij}$, $\sum Q_{ij}$ are calculated active and reactive power injected at bus i, and the expression are the second terms on right-hand side of (3) and (4). P_i^{com} is the power consumed by moto-compressor in gas network which is connected to node i of electricity network, and the power can be calculated by the coupled model in Section IV-A. Q_i^{gen} and Q_i^{load} are reactive power generation and load consumption at bus i, respectively.

Assuming the first bus is chosen to be reference for the voltage angle. Then the unknown vector of state variables is $[X_e] = [\tilde{P}, \theta, V]$. So the nodal active power balance equation (14) is applied to all nodes of electricity network.

III. Gas System Formulation by Considering Multi-type Gas Supply Sources

The mixture of multi-type gas sources leads to the variations of SG and GCV at different parts of the gas network. Hence, the unknown variables for the gas nodes can be SG, GCV and pressure. The reclassified node types are shown in Table I.

TABLE I
THE RECLASSIFIED NODE TYPES WITH THEIR KNOWN AND UNKNOWN VARIABLES OF GAS NETWORK

Node type	Known	Unknown
Slack (Main source)	π, SG, GCV	f
Non-mixed sources	f, SG, GCV	π
Mixed sources	f	π, SG, GCV
Load nodes	$EnergyDemand$	π, SG, GCV

The main source is slack node with known pressure, SG and GCV. The non-mixed sources that are sources connected to the gas nodes without being mixed, hence the injected volume flow, SG and GCV are known. The mixed sources, their injected volume flow are known but the SG and GCV after being mixed as well as pressure are unknown. Load nodes include traditional gas loads and GfG units, whose energy demand are known but nodal pressure, SG and GCV are unknown.

Similar to the power system, when the MSB model is used and the P2G units are worked on participating units mode, the gas output of P2G units also changes with iterative participation factors. Then the variable volume flow of P2G units at node i can be expressed as:

$$f_i^{\text{P2G}} = f_i^{\text{P2G},0} + \zeta_i f(\tilde{P}) \tag{16}$$

where $f_i^{\text{P2G},0}$ is the volume flow injected into node i under the set-point of active power of P2G. $f(\tilde{P})$ is the coupled model between consumd power and generated flow of P2G unit (see Section IV-A). Then the node flow equation with multi-type gas sources that satisfies Kirchhoffs First Law can be written as:

$$\Delta f_i = f_i^{\text{NG}} + f_i^{\text{P2G}} - f_i^{\text{Gload}} - f_i^{\text{GfG}} - \sum_{j=1}^{N_G} f_{ij} = 0 \quad \forall i = 1, 2, \cdots, (N_G - 1) \tag{17}$$

$$f_{ij} = C_{ij} \text{sign}_P(\pi_i, \pi_j) \sqrt{\text{sign}_P(\pi_i, \pi_j) \cdot (\pi_i^2 - \pi_j^2)} \tag{18}$$

where π_i and π_j are pressures at node i and j, respectively. $\mathrm{sign}_P(\pi_i, \pi_j)$ is a sign function of pressures where the value is +1 if $(\pi_i^2 - \pi_j^2) \geq 0$ and -1 otherwise. f_{ij} is volume flow in the pipeline between node i and j. C_{ij} is pipeline coefficient and the formula contains SG, detailed in [26]. f^{NG} is the volume flow of NG injected into node i. f_i^{P2G} is the volume flow injection of gas generated by P2G units. f_i^{Gload} is volume flow demand of gas load at node i, which can be obtained by Energy Demand/GCV$_i$. f_i^{GfG} is the volume flow demand of GfG unit in an electricity network which is connected to node i of the gas network, and the volume flow can be obtained by the coupled model in Section IV-A. N_G is the total number of gas nodes. A slack node with specified reference pressure is set to calculate other unknown node pressures, so (17) is applied to all nodes of gas network, except slack node.

In order to obtain the values of SG and GCV at each node, specific gravity and gross calorific value are modelled as iterative state variables in this paper. The mixed SG and GCV propositions of multiple incoming pipelines are considered according to the mass continuity equation of fluid [23], [27]. Traditional natural gas (NG), hydrogen (H_2) and synthetic natural gas (SNG) are mainly considered in this paper, then the SG and GCV mismatches are expressed as follows:

$$\begin{aligned}
&\Delta SG_i \\
&= SG_i\left(f_i^{\mathrm{NG}} + f_i^{\mathrm{H_2}} + f_i^{\mathrm{SNG}} + \sum_{j=1}^{N_G} \mathrm{sign}_f(f_{ji}) \cdot f_{ji}\right) \\
&\quad - \left[f_i^{\mathrm{NG}} SG_{\mathrm{NG}} + f_i^{\mathrm{H_2}} SG_{H_2} + f_i^{\mathrm{SNG}} SG_{\mathrm{SNG}}\right. \\
&\quad \left. + \sum_{j=1}^{N_G} \mathrm{sign}_f(f_{ji}) \cdot (f_{ji} SG_j)\right] = 0 \\
&\forall i = 1, 2, \cdots, (N_G - 1 - N_{\text{non-mixed}})
\end{aligned} \tag{19}$$

$$\begin{aligned}
&\Delta GCV_i \\
&= GCV_i\left(f_i^{\mathrm{NG}} + f_i^{\mathrm{H_2}} + f_i^{\mathrm{SNG}} + \sum_{j=1}^{N_G} \mathrm{sign}_f(f_{ji}) \cdot f_{ji}\right) \\
&\quad - \left[f_i^{\mathrm{NG}} SG_{\mathrm{NG}} + f_i^{\mathrm{H_2}} GCV_{H_2} + f_i^{\mathrm{SNG}} GCV_{\mathrm{SNG}}\right. \\
&\quad \left. + \sum_{j=1}^{N_G} \mathrm{sign}_f(f_{ji}) \cdot (f_{ji} GCV_j)\right] = 0 \\
&\forall i = 1, 2, \cdots, (N_G - 1 - N_{\text{non-mixed}})
\end{aligned} \tag{20}$$

where SG_i and SG_j are specific gravity of mixed gas flow out of nodes i and j, respectively. GCV_i and GCV_j are gross calorific values of mixed gas flow out of nodes i and j, respectively. $\mathrm{sign}_f(f_{ji})$ is a sign function of gas flow where $\mathrm{sign}_f(f_{ji}) = 1$ if $f_{ji} \geq 0$ and 0 otherwise. $f^{\mathrm{H_2}}, f^{\mathrm{SNG}}$ are volume flow of H_2, SNG injected into node i, respectively. For brevity, the SG and GCV of the leaving gas of a node is the average of all incoming pipelines' gas characteristic considering flows as their weighting factors. It can be expressed by $X_{\mathrm{out}} = \sum(\dot{f}_{\mathrm{in}} X_{\mathrm{in}}) / \sum \dot{f}_{\mathrm{in}}$ which is valid for both SG and GCV. Similarly, the SG and GCV of the source node are known, so the slack node and non-mixed sources nodes are not included in (19)–(20). It is worth noting that if the direction of the gas flow changes and the gas inject into the non-mixed source node, the node type of non-mixed source is converted to load nodes.

IV. A Bi-directional Energy Flow Formulation

A. Interdependencies Between Power System and Gas System

The relationship between the volume flow required and active power output of GfG units can be expressed by:

$$f_i^{\mathrm{GfG}} = \frac{1}{GCV_i}\left(\alpha_i^{\mathrm{GfG}} (P_i^{\mathrm{GfG}})^2 + \beta_i^{\mathrm{GfG}} P_i^{\mathrm{GfG}} + \gamma_i^{\mathrm{GfG}}\right) \tag{21}$$

where α_i^{GfG}, β_i^{GfG} and γ_i^{GfG} are heat rate coefficients of GfG units at node i. It can be found that the volume flow consumed by GfG unit is not only a function of the active power generated but also a function of GCV at node i of the gas network in this paper.

P2G technology converts power into gas via two processes [28]. In the first process, water is electrolyzed into H_2 which can be injected into the gas network in a limit range. For example, the maximum level of H_2 content is 0.1%vol in the UK while this level is petitioned to be raised to 3%vol [9], [29], even up to 17%vol should not cause difficulties [8], [30]. In the second process, H_2 combines CO_2 to form CH_4, known as SNG, can be directly injected into the gas network without restriction. Although the products in the two processes are different, they both take the first process as core. Thus, the universal formula used to express the relationship between consumed power P_i^{P2G} and generated gas flow f_i^{P2G} can be given as:

$$f_i^{\mathrm{P2G}} = \left(\frac{3600 \eta_{\mathrm{P2G}}}{GCV}\right) P_i^{\mathrm{P2G}} \tag{22}$$

where η_{P2G} is the energy conversion efficiency.

Moto-compressors in the gas network are installed to compensate for the drop in pressure of the pipeline. The active power consumed by moto-compressors can be calculated by [6]:

$$P_i^{\mathrm{com}} = \frac{745.7 \times 10^{-6}}{3600} \frac{\lambda_G}{\lambda_G - 1} E_i^{\mathrm{com}} f_{ij}\left(\left(\frac{\pi_j}{\pi_i}\right)^{\frac{\lambda_G - 1}{\lambda_G}} - 1\right) \tag{23}$$

where E_i^{com} is the parameters related to the compressor efficiency, gas compressibility factor and gas temperature at the compressor node. λ_G is the specific heat ratio of gas, which is updated with the change of the gas composition.

B. A Bi-directional Energy Flow Solver

The bi-directional energy flow analysis of integrated power-gas systems are formulated by combining the model of the power system (Section II), the gas system (Section III) and the coupled units including the GfG, P2G and moto-compressor (Section IV-A). Then, a bi-directional energy flow solver (BEFS) incorporating the MSB model and multi-type gas supply sources with iterative SG, GCV and participation factors is implemented. In the BEFS algorithm, the formulated set of nonlinear equations to be solved are given by:

$$\Delta F = [\Delta P \quad \Delta Q \quad \Delta f \quad \Delta SG \quad \Delta GCV]^{\mathrm{T}} = 0 \tag{24}$$

where $\Delta P \in \Re^{N_{\rm E}}$, $\Delta Q \in \Re^{N_{\rm PQ}}$, $\Delta f \in \Re^{N_G-1}$, $\Delta SG \in \Re^{N_G-1-N_{\text{non-mix}}}$ and $\Delta GCV \in \Re^{N_G-1-N_{\text{non-mix}}}$. The state variables to be solvable are:

$$X = [\tilde{P} \;\; \theta \;\; V \;\; \pi \;\; SG \;\; GCV]^{\rm T} \tag{25}$$

where $\tilde{P} \in \Re$, $\theta \in \Re^{N_E-1}$, $V \in \Re^{N_{\rm PQ}}$, $\pi \in \Re^{N_G-1}$, $SG \in \Re^{N_G-1-N_{\text{non-mixed}}}$, $GCV \in \Re^{N_G-1-N_{\text{non-mixed}}}$, respectively. Therefore, the total number of unknown variables is equal to the total number of equations in (24), then the unknown variables of the power-gas system can be solvable.

The nonlinear equations and the unknown state variables are solved iteratively by the Newton-Raphson method. The iterative formula is $X^{(k+1)} = X^(k) - [J^{(k)}]^{-1}\Delta F^{(k)}$ where k is the current iteration, J is the integrated jacobian matrix. For the proposed integrated model, J is expressed by (26).

$$J = \left[\begin{array}{ccc|ccc} \frac{\partial \Delta P}{\partial \tilde{P}} & \frac{\partial \Delta P}{\partial \theta} & \frac{\partial \Delta P}{\partial V} & \frac{\partial \Delta P}{\partial \pi} & \frac{\partial \Delta P}{\partial SG} & 0 \\ 0 & \frac{\partial \Delta Q}{\partial \theta} & \frac{\partial \Delta Q}{\partial V} & 0 & 0 & 0 \\ \hline \frac{\partial \Delta f}{\partial \tilde{P}} & 0 & 0 & \frac{\partial \Delta f}{\partial \pi} & \frac{\partial \Delta f}{\partial SG} & \frac{\partial \Delta f}{\partial GCV} \\ \frac{\partial \Delta SG}{\partial \tilde{P}} & 0 & 0 & \frac{\partial \Delta SG}{\partial \pi} & \frac{\partial \Delta SG}{\partial SG} & 0 \\ \frac{\partial \Delta GCV}{\partial \tilde{P}} & 0 & 0 & \frac{\partial \Delta GCV}{\partial \pi} & 0 & \frac{\partial \Delta GCV}{\partial GCV} \end{array}\right] \tag{26}$$

Note that the first column in (26) exists because of the utilization of MSB model. $\partial \Delta P/\partial \tilde{P}$ is a N_E-dimensional 1-column matrix composed of iterative participation factors ζ and zero elements, where zero elements for non-participating units. $\partial \Delta f/\partial \tilde{P}$ is the derivative of the volume flow mismatches with respect to the active power slack and it is nonzero because the volume flow consumption or injection of participating units varies with the variable active power. Similarly, $\partial \Delta SG/\partial \tilde{P}$ and $\partial \Delta GCV/\partial \tilde{P}$ are derivatives of the SG and GCV mismatches of mixed gas with respect to the active power slack and they are all nonzero because the variable active power affects gas composition in gas network through GfG or P2G units. $\partial \Delta P/\partial \pi$ and $\partial \Delta P/\partial SG$ are nonzero if moto-compressors are loads of the electric network. It is worth noting that $\partial \Delta SG/\partial SG$ and $\partial \Delta GCV/\partial GCV$ are new diagonal items when considering multi-type gas supply sources. Meanwhile, $\partial \Delta f/\partial SG$ and $\partial \Delta f/\partial GCV$ are not zero due to the effect of SG and GCV on volume flow. The value of $\partial \Delta SG/\partial \pi$ and $\partial \Delta GCV/\partial \pi$ are derivatives of the SG and GCV mismatches with respect to the pressure and they are usually very small compared to other nonzero elements of the integrated jacobian matrix. For simplicity, they can be put as zero.

The flow chart of this solution algorithm is shown in Fig. 1. The power sensitivity method can be used as a pre-processing to calculate the actual active power of the participating units in multi-energy flow calculations. The power sensitivity matrix S changes at each ieration and implicitly includes the effects of system parameters and conditions. The initialization of voltage magnitudes, angles and pressures are consistent with [14]. The initial values of the participation factors are $[1, 0, \cdots, 0]^{\rm T}$ to avoid a null diagonal element in the integrated jacobin. The nodal SG and GCV can be initialized at the values of main gas source's SG and GCV. A mismatch tolerance of 10^{-6} is considered.

V. Case Studies

The bi-directional energy flow solver was tested on an integrated IEEE 14-bus power system and a Belgian 20-node system (Fig. 1). For the IEEE 14-bus power system, it has two GfG units (GfG1 at E1 and GfG2 at E2), three wind turbines and three P2G units (P2G1 at E3, P2G2 at E6 and P2G3 at E8) in this paper. The lines parameters and electricity load demands can be obtained in [15]. For the Belgian 20-node gas system [31], the gas well at G1 provides traditional natural gas and serves as a slack node with the reference pressure of 56 bar. SNG are injected into G2, G5, G8, G13 and G14 at a flow

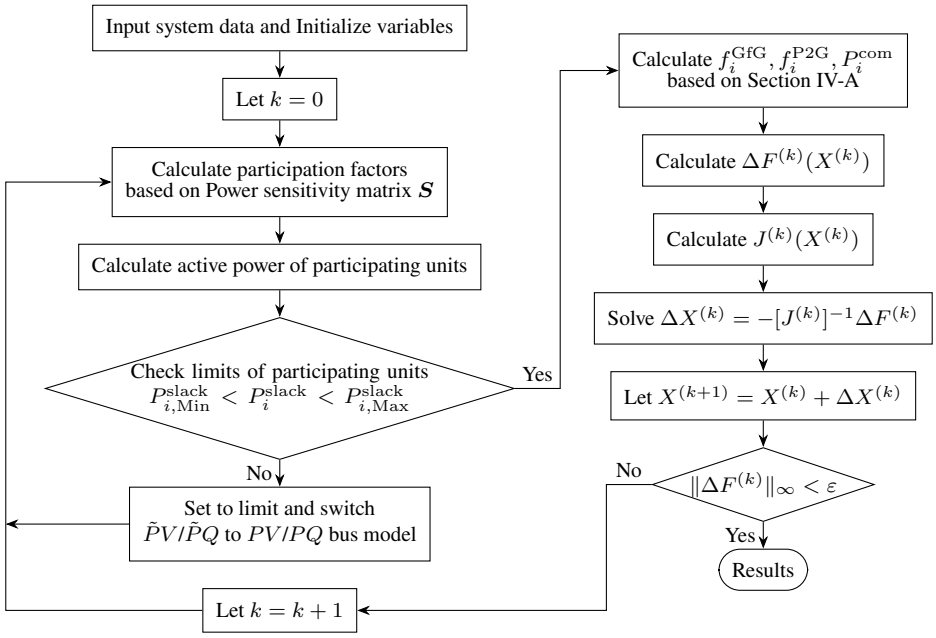

Fig. 1. Flowchart of the solution algorithm.

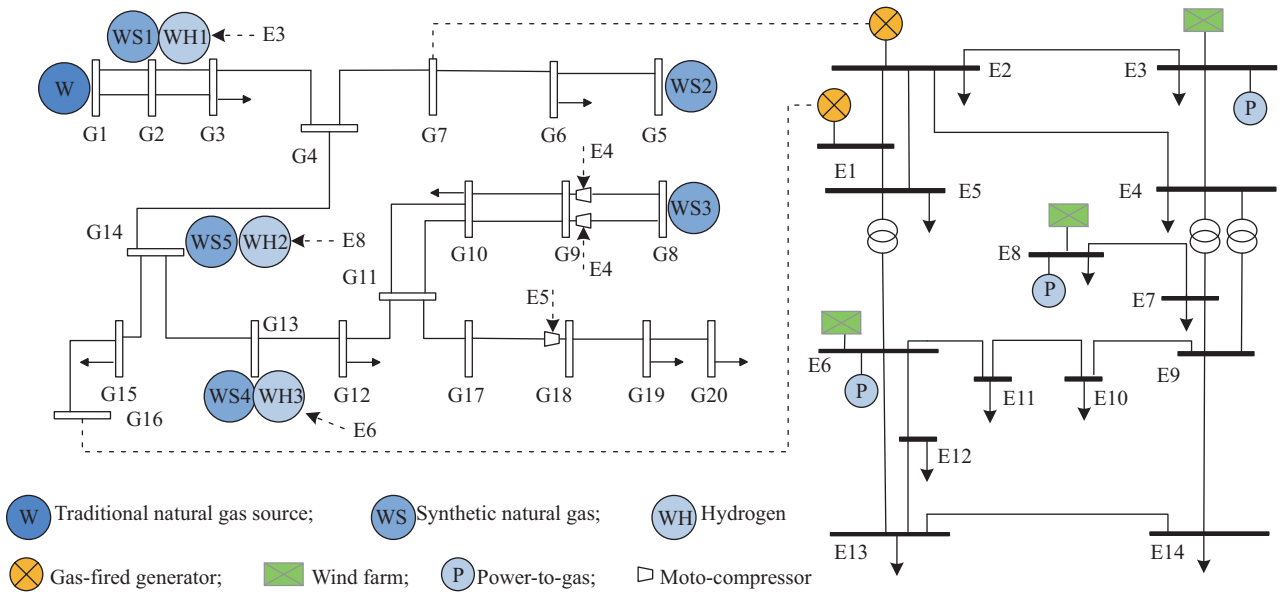

Fig. 2. Integrated IEEE 14-bus system and Belgian 20-node gas system.

rate of 8.4, 2.8, 25.012, 1.2 and 0.96 (Mm^3/h), respectively. And the volume flow of H_2 injected into G2, G13, G14 are 8.4, 1.2, 0.96 (Km^3/h), respectively, 0.1% of the volume flow of SNG injected into each node. It is assumed that there is no gas leakage and the gases are completely mixed without chemical reaction. The pipelines parameters and gas load demands are given in [26]. The SG and GCV of different gas supply sources are shown in Table II. The following seven cases are studied.

TABLE II
SPECIFIC GRAVITY AND GROSS CALORIFIC VALUE OF GAS SOURCES

Gas characteristics	Natural gas (NG)	Synthetic natural gas (SNG)	Hydrogen (H_2)
Specific gravity	0.6048	0.58	0.0696
Gross calorific value (MJ/m^3)	41.04	37.40	12.75

Base case (B-Case): This case represents the conventional energy flow where natural gas as the only source and GfG1 is selected as the single slack bus.

Case 1: Similar to the Base case, but the mixture of multi-type gas supply sources are considered.

Case 2: Similar to Case 1, but all GfG and P2G as participating units are considered. And 5% of the system active power demand as slack variable is compensated by participating units.

Case 3: Similar to Case 2, but 10% of the system active power demand as slack variable is compensated by participating units.

Case 4: Similar to Case 3, but 10% of the system active power demand at end of the electricity network as slack variable is compensated by participating units.

Case 5: Similar to Case 2, but 20% of the system active power demand as slack variable is compensated by participating units.

Case 6: Similar to Case 5, but only GfG units as participating units are considered.

The BEFS algorithm is used for each case, and the case studies are designed to demonstrate the effect of MSB model and multi-type gas supply sources on the steady state equilibrium point of integrated power-gas systems.

A. *Effect of Proposed Multi-Slack Bus Model*

The different results brought by the proposed model are analyzed in the following aspects: 1) participation factors; 2) the active power output of reference bus; 3) the gas output of the slack node; 4) voltage profile; 5) pressure profile; 6) line-pack. The steady-state results obtained are summarized in Figs. 3–8.

1) Participation Factors

The participation factors for the participating units of each case are shown in Fig. 3. The different value of participation factor is represented by the heatmap with different colors. For instance, in the Base Case and Case 1, the bright yellow indicates that the participation factor of GfG1 unit is 1, and the white indicates that the participation factors of other units are 0, this means that only the GfG1 unit is used as the single slack bus, and other units do not participate in slack compensation. Case 2–Case 6 are simulated to further observe the changes of

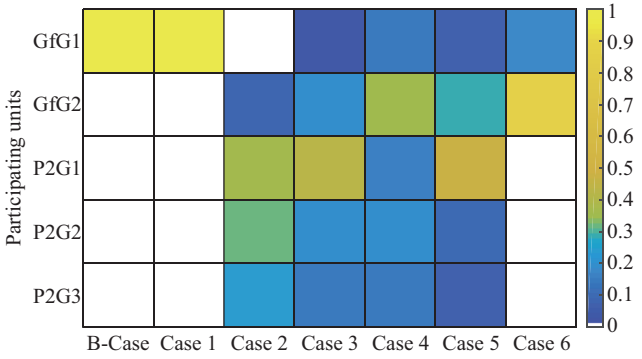

Fig. 3. The participation factors heatmap.

participation factors in the proposed MSB model. The slack in case 2 is mainly compensated by GfG2, P2G1, P2G2 and P2G3. Their participation factors are represented by blue (with the value of 0.0855 and 0.2380, respectively) for the GfG2 and P2G3, and grass-green (with the value of 0.3152) for the P2G2, and yellow-green (with the value of 0.3613) for the P2G1. The slack in Case 3 is compensated by the all participating units, of which P2G1 plays a major role. The slack in Case 4 is compensated by the all participating units but GfG2 plays a major role. By comparing Case 3 and 4, it can be found that the participating units undertake the same slack but have different participation factors. The participation factors of P2G2 and P2G3 in Case 5 have the lower value (with darker blue) than the Case 2-Case 4, because they reach the operational limit. In Case 6, P2G units are not operated as participating units, then GfG2 plays a dominant role. The above results denote that the slack contributed by each participating unit is related to the system conditions, such as the level of active power slack, operational limit, load locations and the generator distribution.

2) The Active Power Output of Reference Bus

Figure 4 shows the active power output of the reference bus in each case. It can be found that the application of the proposed MSB model reduces the active power supplied by the reference bus. If the unit capacity of the reference bus is limited to 1.6 p.u, the system would overload by using SSB model. In addition, the active power output of the reference bus in Case 5 has an additional 2.2% reduction compared to Case 6. The comparing for Case 5 versus Case 6 proves that distributing the active power slack by simultaneously using GfG and P2G units reduces the reference bus output power compared to distributing the active slack by only using GfG units. Furthermore, if the capacity is limited to 1.18 p.u, the system would overload by only using GfG units as participating units. The cases show that the effectiveness of proposed MSB model.

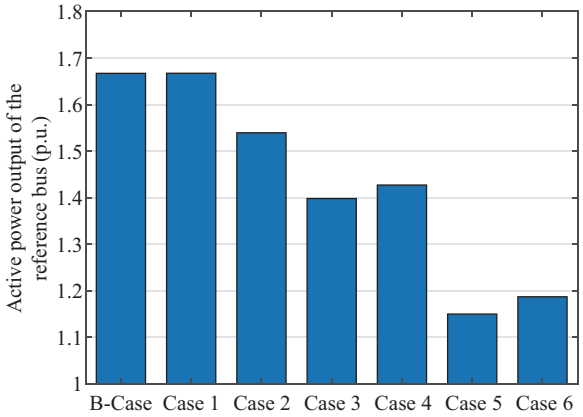

Fig. 4. The active power output of reference bus.

3) The Gas Output of the Slack Node

As shown in Fig. 5, the gas outputs of slack node in Case 2-Case 6 are obviously reduced. This is because the use of MSB model reduces the active power outputs of GfG units, thereby reducing the demands of gas loads. From Fig. 3, the participation factors of the two GfG units in Case 4 are higher

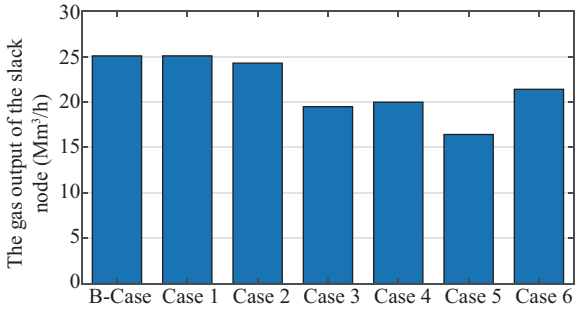

Fig. 5. The gas output of the slack node.

than Case 3, that is, the demands of gas network loads are higher than Case 3, thus the gas output of the slack node is also higher in Case 4. Noting that the participation factors of the P2G units in Case 4 are smaller than Case 3, that means the active power inputs of P2G units are higher in Case 4, so the volume flow of H_2 injected into the gas network is higher in Case 4. Since the H_2 content in the gas network is obviously less than 0.1%, the higher injection of H_2 sources has less impact on the gas output of slack node than the higher demands of gas loads. Similarly, the comparison between Case 5 and Case 6. The results show that the use of MSB model affects the slack node outputs of both electricity and gas networks.

4) Voltage Profile

The voltage profile is increased by using the MSB model as shown in Fig. 6. By comparing Case 1 and other Cases, it can be found that the maximum voltage difference is at Bus-14, and the value of the voltage difference is 0.0166 pu at most, which indicates that distributing the active slack by using multi-slack bus increases the voltage profile compared to using the single slack bus. In addition, the voltage at bus 4, 5 and 7 in Case 5 are increased by 0.001 pu at most compared to Case 6. The comparison of Case 5 versus Case 6 indicates that distributing the active slack by simultaneously using GfG and P2G units increases the voltage profile compared with only using GfG units. This is because the active power slack is distributed by all participating units and the GfG1 unit would not need to transmit long distance to maintain power balance. At the same time, the active power demands of P2G units are released, that is, the power demands of the whole network are also decreased.

5) Pressure Profile

Just like voltage is an important factor for electricity network, pressure is an important factor for the safety of gas network. Fig. 7 reports the pressure of each case. The pressure profile is higher when using the MSB model. By comparing Case 1 and other Cases, it can be found that the maximum pressure difference is at the end of the gas network, node-20, and the value of the pressure difference is 37.952 bar at most, which is increased by 814.2% compared to Case 1. In addition, taking critical node-20 as an example, the pressure in Case 5 has been increased by 6.8272 bar (increased by 19.078%) compared to Case 6, the comparison of Case 5 versus Case 6 indicates that distributing the active slack by simultaneously using GfG and P2G as participating units can

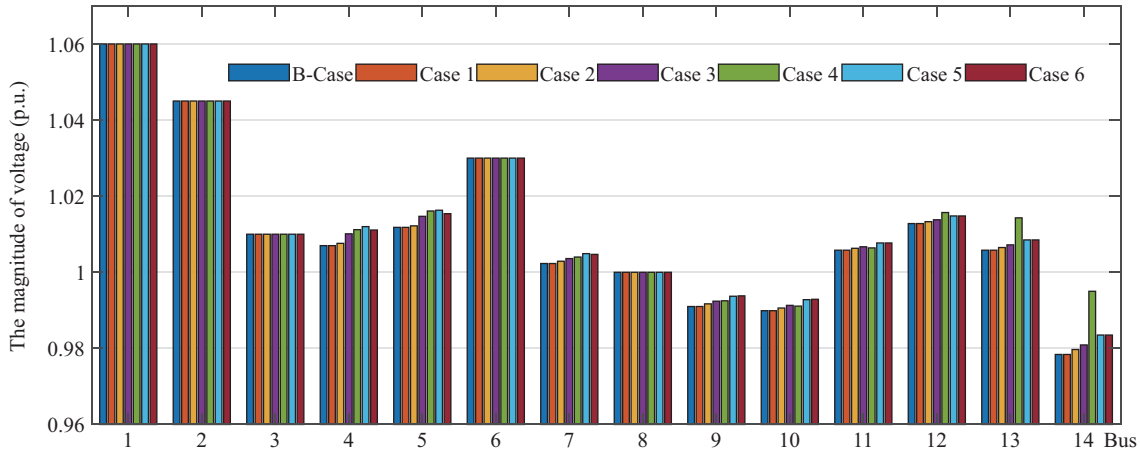

Fig. 6. Comparing the changes of bus voltage for different cases.

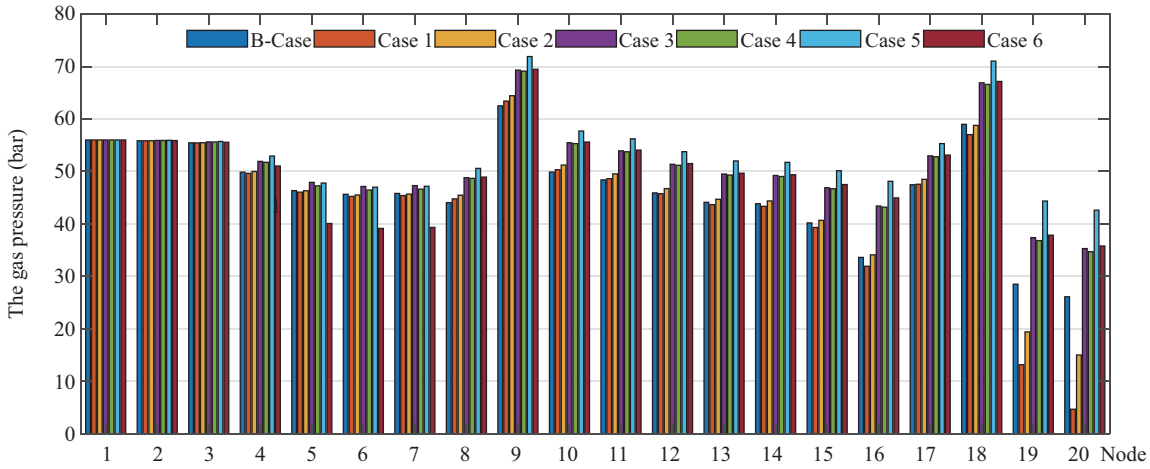

Fig. 7. Comparing the changes of node pressure for different cases.

increase the pressure profile. According to the results, the use of MSB model not only reduces the active power output of the reference bus, but also greatly reduces the burden of the gas network for power balancing. Then the pressure profile are increased, which is more helpful to the reliable operation of gas network.

6) Line-pack

Line-pack plays a major role in providing flexibility and reliability to the natural gas system [32], and it is an important indicator for subsequent optimization and scheduling. This paper gives the steady-state line-pack of the end of the gas network pipeline based on the formula in [33], as shown in Fig. 8. It can be seen that the value of line-pack changes with the gas source composition, the level of the active power slack and the selection of the slack buses. And the line-pack of the system with MSB model is larger than that without MSB model. Meanwhile, the line-pack of the system with both GfG and P2G unit as participating units is larger than that with only GfG units. The cases show that the effectiveness of proposed MSB model for gas network.

From the results, we can conclude that system conditions affect the participating units' slack contribution. Then the active power output of reference bus with a MSB model are

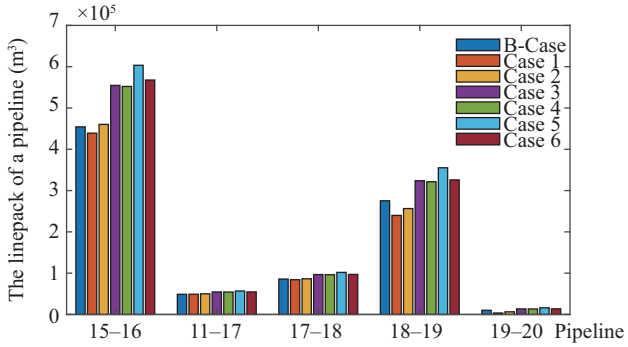

Fig. 8. The line-pack of pipelines at the end of the gas network.

smaller than the output with a SSB or DSB model. That is, the proposed MSB model can help to reduce the burden of the slack bus, thereby helping the system to tackle the problem of the capacity limitation of the slack bus. Meanwhile, the profile of voltage and pressure as well as the line-pack under steady-state are all higher in the system with MSB model.

B. Effect of Multi-type Gas Supply Sources

Taking the steady-state results of the Base case and Case

1 as examples, the effect of multi-type gas supply sources on integrated power-gas systems are analyzed. In the Base Case, the volume flow of H_2 or SNG injected into the gas network are converted to the volume flow of equivalent natural gas which carries the same amount of energy. The gas flow demand can be expressed directly by flow rate and do not change with iterations. In Case 1, H_2 and SNG are directly injected into gas network and mixed with traditional natural gas. The SG, GCV and volume flow of demand are calculated during per-iterative. Results obtained are summarized in Tables III and IV.

Table III summarizes the gas supply, demand by gas loads as well as GfG units, nodal pressure, nodal SG and GCV. The second column is the volume flow supply of equivalent natural gas, and the third column is the sum of volume flows supplied by H_2, SNG and NG at each node. In Case 1, the mixture of H_2, SNG and NG reduces the values of SG and GCV at all nodes except node-1, which can be seen from the last 4 columns. Therefore, in order to meet the energy demand, the volume flow demands of gas loads and GfG units become higher compared to B-Case, which are shown in columns 4–7. It is also proved from the product of GCV and volume flow demand, for instance, $GCV_{\text{B-Case}} \times Demand_{\text{B-Case}}/GCV_{\text{Case 1}} = Demand_{\text{Case 1}}$ are satisfied at all nodes. Consequently, the pressure drops are increased with a higher volume flow demand, and the nodal pressure profile is decreased. Taking critical node 20 as an example, a 9.73% increase in volume flow demand and a 82.15% decrease in pressure when considering the mixture of multi-type gas supply sources. Finally, it is easy to verify that the total injected volume flow in each method is equal to the total consumed.

Table IV reports pipeline coefficients C_{ij}, volume flows and the consumption of moto-compressors for several pipelines. The C_{ij} are generally larger in Case 1. This is because the gas mixture has a lower SG than traditional natural gas (0.6048) and C_{ij} increase with the decrease of SG. At the same time, the higher volume flow of pipeline transmission in Case 1 increases the electric power consumed by the moto-compressor, which are increased by 9.67%, 10.38% and 9.91% compared to B-Case, respectively. The results show that, the mixture of multi-type gas supply sources affects the final energy flow results of both gas and electricity network.

TABLE IV
PIPELINES COEFFICIENTS, FLOWS AND CONSUMPTION OF MOTO-COMPRESSOR

From	To	C_{ij}		Gas flow (Mm^3/h)		Compressor (KW)	
		B-Case	Case 1	B-Case	Case 1	B-Case	Case 1
8	9	2.7066	2.7639	20.3148	22.2920	121.66	133.42
8	9	0.3303	0.3372	2.4788	2.7200	14.84	16.38
17	18	0.0805	0.0822	2.141	2.3494	34.30	37.70

VI. CONCLUSION

This paper builds a system model of an integrated power-gas system. The model of a multi-slack bus for bi-directional energy flow analysis is proposed to overcome the shortcomings of adjusting active power balance only by single gas-fired unit and the great burden of slack bus on the gas network. In addition, this paper further considers the influence of network characteristics on participation factors. Results show that the slack contributed by each participating units is related to the system conditions. Meanwhile, the application of the multi-slack bus model positively impacts the steady-state operation of the integrated power-gas systems. The results can provide the basis and insights for the subsequent optimization and control of integrated systems. Moreover, the gas characteristics SG and GCV are firstly modeled as iterative state variables in bi-directional energy flow analysis. The consideration of mixed gas sources problem can help to provide correct data for higher level research.

It is worth noting that when the network status changes, the slow dynamic characteristic of the natural gas system may require several hours to transit the system to a new steady state. This operational process can provide dispatchers with

TABLE III
GAS SUPPLY, DEMAND, NODAL PRESSURES, SPECIFIC GRAVITY AND GROSS CALORIFIC VALUE OF GAS NETWORK

Node	Source (Mm^3/h)		Demand (Mm^3/h)		GfG (Mm^3/h)		Pressure (bar)		SG		GCV (MJ/m^3)	
	B-Case	Case 1	B-Case	Case 1	B-Case	Case 1	B-Case	Case 1	B-Case	Case 1	B-Case	Case 1
1	25.0696	25.0728	0	0	0	0	56	56	0.6048	0.6048	41.04	41.04
2	7.6576	8.4084	0	0	0	0	55.8466	55.8466	0.6048	0.5984	41.04	40.1197
3	0	0	3.918	4.0079	0	0	55.4525	55.4384	0.6048	0.5984	41.04	40.1197
4	0	0	0	0	0	0	49.8583	49.6316	0.6048	0.5984	41.04	40.1197
5	2.5517	2.8	0	0	0	0	46.3431	46.0524	0.6048	0.58	41.04	37.4
6	0	0	4.034	4.3163	0	0	45.6438	45.2388	0.6048	0.5865	41.04	38.3554
7	0	0	0	0	7.9435	8.1257	45.8039	45.4060	0.6048	0.5984	41.04	40.1197
8	22.7936	25.012	0	0	0	0	44.0504	44.7720	0.6048	0.58	41.04	37.4
9	0	0	0	0	0	0	62.5051	63.4170	0.6048	0.58	41.04	37.4
10	0	0	6.365	6.9845	0	0	49.8776	50.3254	0.6048	0.58	41.04	37.4
11	0	0	0	0	0	0	48.3886	48.6177	0.6048	0.58	41.04	37.4
12	0	0	2.12	2.3263	0	0	45.9063	45.7536	0.6048	0.58	41.04	37.4
13	1.0939	1.2012	0	0	0	0	44.1102	43.6657	0.6048	0.58	41.04	37.398
14	0.8752	0.96096	0	0	0	0	43.8373	43.3471	0.6048	0.5903	41.04	38.9244
15	0	0	6.848	7.2202	0	0	40.1865	39.3202	0.6048	0.5903	41.04	38.9244
16	0	0	0	0	26.6720	28.1251	33.6067	31.9236	0.6048	0.5903	41.04	38.9244
17	0	0	0	0	0	0	47.4679	47.5580	0.6048	0.58	41.04	37.4
18	0	0	0	0	0	0	58.9779	57.0212	0.6048	0.58	41.04	37.4
19	0	0	0.222	0.2436	0	0	28.5066	13.1577	0.6048	0.58	41.04	37.4
20	0	0	1.919	2.1058	0	0	26.1057	4.6600	0.6048	0.58	41.04	37.4

more decision-making information. Therefore, on the basis of this paper, a multi-period operation analysis of the integrated power-gas systems considering dynamic characteristic will be presented in a subsequent paper.

REFERENCES

[1] R. Wang, Q. Y. Sun, D. Z. Ma, and X. G. Hu, "Line impedance cooperative stability region identification method for grid-tied inverters under weak grids," *IEEE Transactions on Smart Grid*, vol. 11, no. 4, pp. 2856–2866, Jul. 2020, doi: 10.1109/TSG.2020.2970174.

[2] N. Zhang, Q. Y. Sun, J. W. Wang, and L. X. Yang, "Distributed adaptive dual control via consensus algorithm in the energy internet," *IEEE Transactions on Industrial Informatics*, vol. 17, no. 7, pp. 4848–4860, Jul. 2021, doi: 10.1109/TII.2020.3031437.

[3] Q. Y. Sun, N. Zhang, S. You, and J. W. Wang, "The dual control with consideration of security operation and economic efficiency for energy hub," *IEEE Transactions on Smart Grid*, vol. 10, no. 6, pp. 5930–5941, Nov. 2019.

[4] B. Odetayo, M. Kazemi, J. MacCormack, W. D. Rosehart, H. Zareipour, and A. R. Seifi, "A chance constrained programming approach to the integrated planning of electric power generation, natural gas network and storage," *IEEE Transactions on Power Systems*, vol. 33, no. 6, pp. 6883–6893, Nov. 2018.

[5] Massachusetts Institute of Technology, *The Future of Natural Gas*: *An Interdisciplinary MIT Study*, Cambridge: Massachusetts Institute of Technology, 2011.

[6] S. Schiebahn, T. Grube, M. Robinius, V. Tietze, B. Kumar, and D. Stolten, "Power to gas: Technological overview, systems analysis and economic assessment for a case study in Germany," *International Journal of Hydrogen Energy*, vol. 40, no. 12, pp. 4285–4294, Apr. 2015.

[7] X. T. Xing, J. Lin, Y. H. Song, Y. Zhou, S. J. Mu, and Q. Hu, "Modeling and operation of the power-to-gas system for renewables integration: a review," *CSEE Journal of Power and Energy Systems*, vol. 4, no. 2, pp. 168–178, Jun. 2018.

[8] M. Qadrdan, M. Abeysekera, M. Chaudry, J. Z. Wu, and N. Jenkins, "Role of power-to-gas in an integrated gas and electricity system in Great Britain," *International Journal of Hydrogen Energy*, vol. 40, no. 17, pp. 5763–5775, May 2015.

[9] S. Clegg and P. Mancarella, "Integrated modeling and assessment of the operational impact of power-to-gas (P2G) on electrical and gas transmission networks," *IEEE Transactions on Sustainable Energy*, vol. 6, no. 4, pp. 1234–1244, Oct. 2015.

[10] D. X. Wang, J. Qiu, K. Meng, X. D. Gao, and Z. Y. Dong, "Coordinated expansion co-planning of integrated gas and power systems," *Journal of Modern Power Systems and Clean Energy*, vol. 5, no. 3, pp. 314–325, May 2017.

[11] H. Khani, N. El-Taweel, and H. E. Z. Farag, "Power congestion management in integrated electricity and gas distribution grids," *IEEE Systems Journal*, vol. 13, no. 2, pp. 1883–1884, Jun. 2019.

[12] T. Jiang, H. W. Deng, L. Q. Bai, R. F. Zhang, X. Li, and H. H. Chen, "Optimal energy flow and nodal energy pricing in carbon emission-embedded integrated energy systems," *CSEE Journal of Power and Energy Systems*, vol. 4, no. 2, pp. 179–187, Jun. 2018.

[13] S. Chen, Z. N. Wei, G. Q. Sun, D. Wang, and H. X. Zang, "Steady state and transient simulation for electricity-gas integrated energy systems by using convex optimisation," *IET Generation, Transmission & Distribution*, vol. 12, no. 9, pp. 2199–2206, May 2018.

[14] A. Martinez-Mares and C. R. Fuerte-Esquivel, "A unified gas and power flow analysis in natural gas and electricity coupled networks," *IEEE Transactions on Power Systems*, vol. 27, no. 4, pp. 2156–2166, Nov. 2012.

[15] A. Shabanpour-Haghighi and A. R. Seifi, "An integrated steady-state operation assessment of electrical, natural gas, and district heating networks," *IEEE Transactions on Power Systems*, vol. 31, no. 5, pp. 3636–3647, Sep. 2016.

[16] Q. Zeng, J. K. Fang, J. H. Li J, and Z. Chen, "Steady-state analysis of the integrated natural gas and electric power system with bi-directional energy conversion," *Applied Energy*, vol. 184, pp. 1483–1492, Dec. 2016.

[17] Y. Hu, H. R. Lian, Z. H. Bie, and B. R. Zhou, "Unified probabilistic gas and power flow," *Journal of Modern Power Systems and Clean Energy*, vol. 5, no. 3, pp. 400–411, May 2017.

[18] A. G. Exposito, J. L. M. Ramos, and J. R. Santos, "Slack bus selection to minimize the system power imbalance in load-flow studies," *IEEE Transactions on Power Systems*, vol. 19, no. 2, pp. 987–995, May 2004.

[19] M. Chertkov, S. Backhaus, and V. Lebedev, "Cascading of fluctuations in interdependent energy infrastructures: gas-grid coupling," *Applied Energy*, vol. 160, pp. 541–551, Dec. 2015.

[20] Z. Qiao, Q. L. Guo, H. B. Sun, Z. G. Pan, Y. Q. Liu, and W. Xiong, "An interval gas flow analysis in natural gas and electricity coupled networks considering the uncertainty of wind power," *Applied Energy*, vol. 201, pp. 343–353, Sep. 2017.

[21] N. N. Cai and A. R. Khatib, "A universal power flow algorithm for industrial systems and microgrids—Active Power," *IEEE Transactions on Power Systems*, vol. 34, no. 6, pp. 4900–4909, Nov. 2019.

[22] E. J. Weber, *Interchangeability of Fuel Gases*, New York: The Industrial Press, 1965.

[23] M. Abeysekera, J. Wu, N. Jenkins, and M. Rees, "Steady state analysis of gas networks with distributed injection of alternative gas," *Applied Energy*, vol. 164, pp. 991–1002, Feb. 2016.

[24] W. L. Wang, D. Wang, H. J. Jia, Z. Y. Chen, B. Q. Guo, H. M. Zhou, and M. H. Fan, "Steady state analysis of electricity-gas regional integrated energy system with consideration of NGS network status," *Proceedings of the CSEE*, vol. 37, no. 5, pp. 1293–1304, 2017.

[25] D. Choi, J. W. Park, and S. H. Lee, "Virtual multi-slack droop control of stand-alone microgrid with high renewable penetration based on power sensitivity analysis," *IEEE Transactions on Power Systems*, vol. 33, no. 3, pp. 3408–3417, May 2018.

[26] D. de Wolf and Y. Smeers, "The gas transmission problem solved by an extension of the simplex algorithm," *Management Science*, vol. 46, no. 11, pp. 1454–1465, Nov. 2000.

[27] K. Kostúr and J. Kačur, "Indirect measurement of syngas calorific value," in *Proceedings of the 2015 16th International Carpathian Control Conference* (*ICCC*), Szilvasvarad: IEEE, 2015, pp. 229–234.

[28] M. Götz, J. Lefebvre, F. Mörs, A. Mcdaniel Koch, F. Graf, S. Bajohr, R. Reimert, and T. Kolb, "Renewable power-to-gas: a technological and economic review," *Renewable Energy*, vol. 85, pp. 1371–1390, Jan. 2016.

[29] UK Hydrogen and Fuel Cell Association, Power to Gas: Energy Storage and Methanation Webinar, 2014.

[30] NaturalHy. Using the existing natural gas system for hydrogen. 2009. Available: https://vdocuments.net/using-the-existing-natural-gas-system-for-hydrogen.html?page=1

[31] C. M. Correa-Posada and P. Sánchez-Martín, "Integrated power and natural gas model for energy adequacy in short-term operation," *IEEE Transactions on Power Systems*, vol. 30, no. 6, pp. 3347–3355, Nov. 2015.

[32] D. W. Chen, Z. J. Bao, and L. Wu, "Integrated coordination scheduling framework of electricity-natural gas systems considering electricity transmission $N-1$ contingencies and gas dynamics," *Journal of Modern Power Systems and Clean Energy*, vol. 7, no. 6, pp. 1422–1433, Mar. 2019.

[33] S. Clegg and P. Mancarella, "Integrated electrical and gas network flexibility assessment in low-carbon multi-energy systems," *IEEE Transactions on Sustainable Energy*, vol. 7, no. 2, pp. 718–731, Apr. 2016.

Yujia Huang received the B.S. degree in Electrical Engineering and Automation, the M.Sc. degree in Power Systems and Automation, and the Ph.D. degree in Electrical Engineering from Northeastern University, Shenyang, China, in 2018, 2020 and 2024, respectively. From 2023 to 2024, she was a visiting Ph.D. student in Energy Department in Aalborg University, Denmark. Her research interests include modeling, energy flow analysis and operation assessment of integrated energy systems.

Qiuye Sun received the Ph.D. degree in Control Science and Engineering from Northeastern University, Liaoning, China in 2007. He is currently a Full Professor with Northeastern University. He has authored or coauthored over 200 papers, authorized over 100 invention patents, and published over 10 books or textbooks. He is an IET Fellow and an Associate Editor of *IEEE Transactions on Neural Networks and Learning Systems, IET Cyber Physical Systems, CSEE Journal of Power and Energy Systems, IEEE/CAA Journal of Automatica Sinica, International Transactions on Electrical Energy Systems*, and etc. His current research interests include optimization analysis technology of power distribution network, network control of Energy Internet, integrated energy systems and microgrids.

Zhang Ning received the B.S. degree in Electrical Engineering from the Hebei University, China, in 2015, and the M.S. degree in Electrical Engineering from the Northeastern University, Shenyang, in 2017. He is currently pursuing his Ph.D. degree in the School of Information Science and Engineering, Northeastern University, China. His research interests are scheduling strategy of energy hub, security operation of multi-carrier energy system and energy trading.

Rui Wang received the B.S. degree in Electrical Engineering and Automation in 2016 from Northeastern University, Shenyang, China, where he is currently working toward the Ph.D. degree in Power Electronics and Power Drive. Since 2019, he has become a visiting scholar with the Energy Research Institute, Nanyang Technological University, Singapore. He has authored or coauthored over 40 papers, authorized over 10 invention patents. He serves as a Review Editor for Frontiers in Energy Research. His research interest focuses on modeling of distributed renewable energy source in microgrid, stability analysis approach and stabilizing control strategy for microgrid, smart grid, and etc.